Studies of Amyloid-Like Fibrillogenesis through β-Sheet-Mediated Self-Assembly of Short Synthetic Peptides

by **Anita Dutt**[a]), **Elinor C. Spencer**[b]), **Judith A. K. Howard**[b]), and **Animesh Pramanik***[a])

[a]) Department of Chemistry, University of Calcutta, 92, A. P. C. Road, Kolkata-700009, India (phone: +91-33-24841647; fax: +91-33-23519755; e-mail: animesh_in2001@yahoo.co.in)

[b]) Department of Chemistry, University of Durham, South Road, Durham, UK-DH1 3LE

Three structurally different types of small peptides, namely, *i*) Boc-Ile-Aib-Ile-OMe (Aib = α-aminoisobutyric acid), *ii*) Boc-Xx-*m*-aminobenzoic acid (Xx = β-Ala and γ-aminobutyric acid), and *iii*) Boc-Xx-*m*-nitroaniline, were found to exhibit β-sheet-mediated fibrillogenesis in the solid state, revealed by FT-IR, single-crystal X-ray diffraction, and FE-SEM studies. Interestingly, the fibrils grown from peptides **2** and **3** were found to bind with the physiological dye Congo red, a characteristic feature of amyloid fibrils.

Introduction. – Currently, considerable research has been directed towards designing and constructing suitable peptide subunits, which can self-assemble into supramolecular helices [1–3] and β-sheets [4–10]. Peptide-based supramolecular β-sheets are important for their numerous potential applications in material [11][12] and biological sciences [13][14]. They are also utilized in fabricating nano-biomaterials [15–21]. Sometimes, self-aggregating, β-sheet-forming peptides create fibrous networks that can trap solvent molecules to form gels [22]. Under suitable conditions, they can also provide molecular scaffolds for growing neurons and cartilage [23][24]. It has been established that β-sheet-driven aggregation of misfolded proteins is responsible for various neurodegenerative diseases such as *Alzheimer*'s disease [25–28], *Parkinson*'s disease [29][30], and prion-related diseases [31][32].

The design and construction of supramolecular β-sheets is important for a better understanding of the peptide self-aggregation mechanism. Therefore, in this study, we have chosen three different types of peptides to explore the self-assembly mechanism in the solid state (*Fig. 1*). The tripeptide Boc-Ile-Aib-Ile-OMe (**1**), which incorporates the helicogenic Aib (α-aminoisobutyric acid), was expected to adopt a bent structural self-assembling subunit. In peptides **2**, Boc-β-Ala-*m*-ABA (*m*-ABA = *m*-aminobenzoic acid), and **3**, Boc-γ-Abu-*m*-ABA (γ-Abu = γ-aminobutyric acid), the ω-amino acids β-Ala and γ-Abu, known for adopting extended conformations [4][33], were attached to *m*-ABA, a template molecule to create a β-sheet-like structure through intermolecular H-bonding. In peptides **4**, Boc-β-Ala-*m*-NA (*m*-NA = *m*-nitroaniline), and **5**, Boc-γ-Abu-*m*-NA, *m*-ABA of peptides **2** and **3** was replaced by *m*-NA, to explore the influence of the NO_2 group on the self-assembling process. All the peptides were synthesized by conventional solution-phase methodology, and their structures were determined by single-crystal X-ray diffraction studies. The morphological studies of the

dried fibrous materials generated from **1**–**5** were carried out with field-emission scanning electron microscopy (FE-SEM).

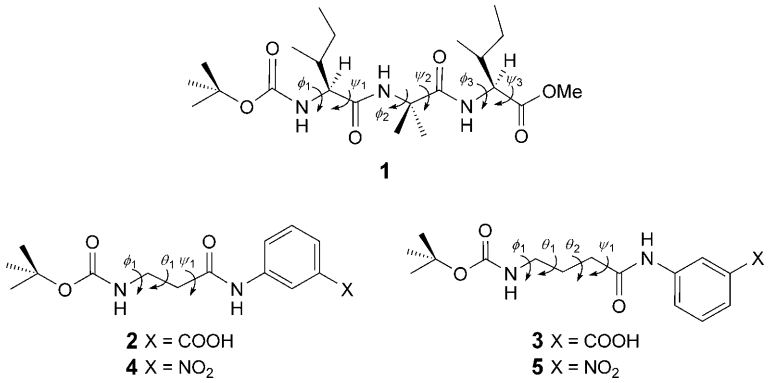

Fig. 1. *Schematic representation of peptides* **1**–**5**

Results and Discussion. – *Solid-State FT-IR Studies.* Solid state FT-IR is a useful tool for obtaining preliminary information about the peptide conformation. In the solid state (KBr matrix), the peptides **1**–**5** showed intense bands at 3326–3387 cm^{-1}, indicating the presence of strongly H-bonded NH groups (*Fig. 2*). Characteristic IR data for all the peptides are listed in *Table 1*. The absence of a band attributable to free NH groups (over 3430 cm^{-1}) indicated that all the NH groups in **1**–**5** were involved in intermolecular H-bonding. The CO stretching band at *ca.* 1667–1696 cm^{-1} (amide I), and the NH bending peak near 1535 cm^{-1} (amide II) suggested the presence of intermolecular H-bonded supramolecular β-sheet-like conformations for all the peptides in the solid state (*Fig. 2*) [34–36]. Therefore, from the solid-state FT-IR data, it can be concluded that all the peptides formed intermolecular H-bonded β-sheet-like structures. To obtain detailed information about the intermolecular H-bonding networks and self-assembly mechanisms, single-crystal X-ray diffraction studies were carried out.

Table 1. *Characteristic Frequences* [cm^{-1}] *of IR Absorption Spectra Obtained from Peptides* **1**–**5** *in the Solid State* (KBr pellets; *s*, strong signal; *m*, medium signal)

Peptide	CO stretch	NH bend	NH stretch
Boc-Ile-Aib-Ile-OMe (**1**)	1667 (*s*)	1523 (*s*)	3387 (*m*), 3320 (*s*)
Boc-β-Ala-*m*-ABA (**2**)	1689 (*s*)	1535 (*m*)	3343 (*s*)
Boc-γ-Abu-*m*-ABA (**3**)	1687 (*s*)	1537 (*m*)	3326 (*s*)
Boc-β-Ala-*m*-NA (**4**)	1696 (*s*)	1546 (*m*)	3326 (*s*)
Boc-γ-Abu-*m*-NA (**5**)	1680 (*s*)	1532 (*s*)	3357 (*s*)

Single-Crystal X-Ray Diffraction Studies. The colorless, orthorhombic crystals of peptide **1** were obtained from an acetone/H_2O mixture by slow evaporation. The molecule crystallized in space group $P2_12_12_1$ with one molecule in the asymmetric unit. A diagram of **1** is presented in *Fig. 3*. The incorporation of helicogenic Aib created a

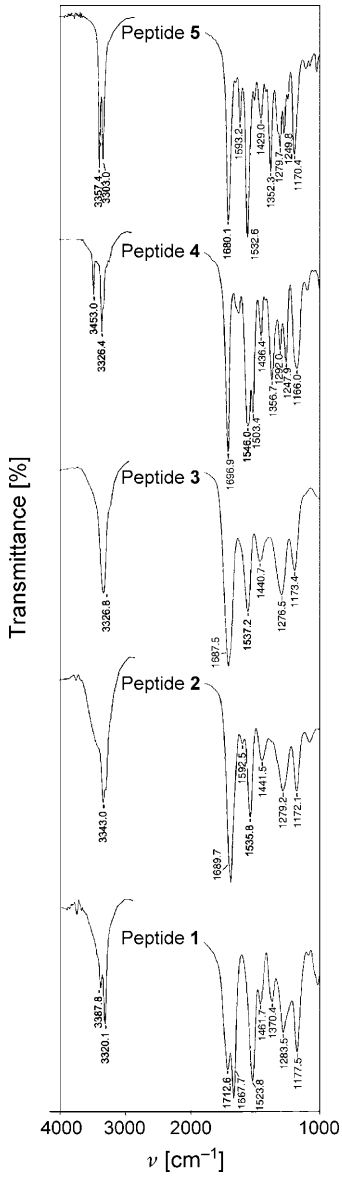

Fig. 2. *FT-IR Spectra of peptides* **1**–**5** *in the regions 3000–4000 and 1000–2000 cm*$^{-1}$

bent structure, where the backbone torsion angles (ϕ, ψ) were: within Ile(1) ϕ_1, $-123.7(2)^\circ$ and ψ_1, $165.7(2)^\circ$; within Aib(2) ϕ_2, $57.2(3)^\circ$ and ψ_2, $38.4(2)^\circ$; and within Ile(3) ϕ_3, $-124.2(2)^\circ$ and ψ_3, $163.4(2)^\circ$ (*Table 2*). The structure corresponded to a distorted type II β-turn conformation with Ile(1) and Aib(2) occupying the $i+1$ and $i+2$ positions, respectively. Due to large deviations of the backbone torsion angles (ϕ, ψ) from the ideal values for a type II β-turn conformation (ϕ_1, -60° and ψ_1, 120°; ϕ_2, 80°

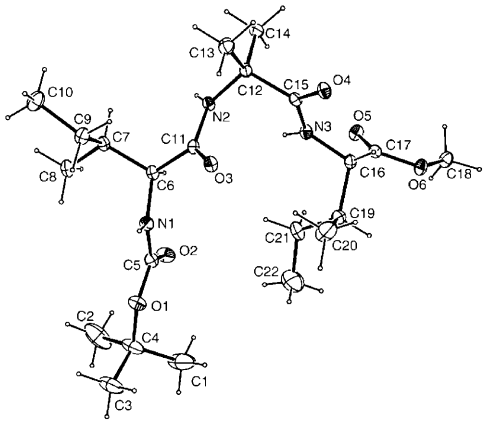

Fig. 3. *ORTEP Diagram of peptide* **1** *with atom-numbering scheme.* Thermal ellipsoids are drawn at the 25% probability level.

Table 2. *Selected Backbone Torsion Angles* [°]

Residues	ϕ_1	ψ_1	θ_1	ϕ_2	ψ_2	ϕ_3	ψ_3
Peptide **1**	−123.7(2)	165.7(2)		57.2(3)	38.4(2)	−124.2(2)	163.4(2)
Peptide **2**							
2A	86.1(6)	81.4(5)	156.9(4)				
2B	−112.5(5)	−86.2(5)	−164.8(4)				
2C	−80.5(6)	−101.3(5)	−157.4(4)				
Peptide **4**	−136.4(2)	140.1(2)	173.4(2)				

and ψ_2, 0°), the turn conformation was unable to permit the formation of any intramolecular H-bonds.

The bent structure of peptide **1** molecules were regularly inter-linked *via* intermolecular H-bonds between the Ile(1) NH moiety of one molecule and the Ile(3) C=O group of another molecule (N1−H1···O5, 2.18 Å) to create a semi-cylindrical structure parallel to the crystallographic *a*-axis (*Fig. 4* and *Table 3*). It was also observed that the Aib(2) NH group of each turn was further H-bonded to an Aib(2) C=O group of a neighboring turn (N2−H2···O4, 2.11 Å) along the crystallographic *b*-axis. As a result, the parallel semi-cylindrical structures were connected to produce a corrugated β-sheet structure along the crystallographic *b*-axis (*Figs. 4* and *5*).

The colorless, triclinic crystals of peptide **2** were grown from an acetone/toluene mixture. The space group is *P*1 with three molecules in the asymmetric unit. A diagram of one of the isomers of **2** is shown in *Fig. 6*. All three molecules adopted extended conformations with similar backbone torsion angles at β-Ala, *e.g.*, in **2A**: ϕ_1, 86.1(6)°; θ_1, 156.9(4)°; ψ_1, 81.4(5)° (*Table 2*). The molecules were self-assembled through intermolecular H-bonds, to create parallel layers of supramolecular β-sheets (*Fig. 7*). In each layer, the molecules were arranged in an antiparallel fashion, so that the *m*-

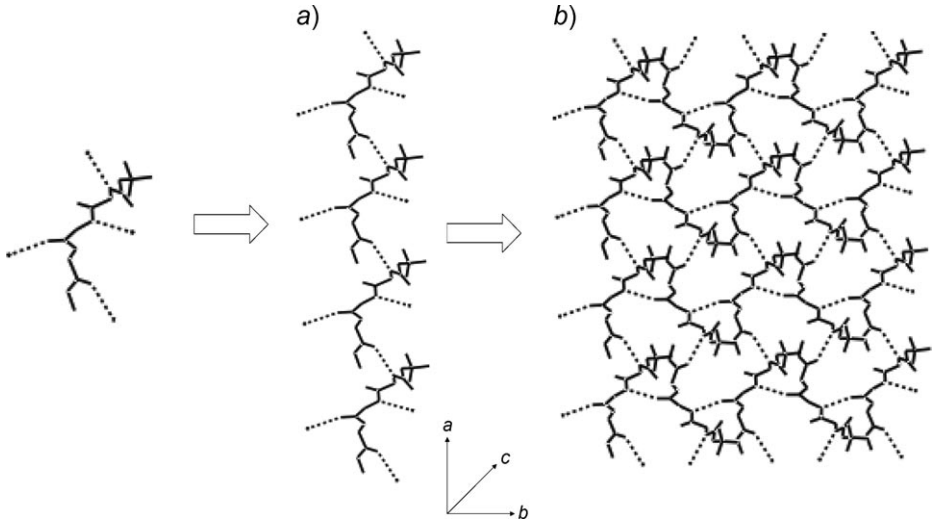

Fig. 4. *Packing diagrams of peptide* **1** *showing* a) *the formation of semi-cylindrical structures parallel to the crystallographic* a-*axis and* b) *the self-association of turns parallel to the crystallographic* b-*axis, forming a layer of β-sheet*. Side chains of amino acids and H-atoms are omitted for clarity.

Table 3. *H-Bonding Parameters for Peptides* **1**, **2**, *and* **4**

D–H···A	H···A [Å]	D···A [Å]	D–H···A [°]
Peptide **1**			
N1–H1···O5^{i}	2.18	3.032(2)	164.31
N2–H2···O4^{ii}	2.11	2.949(2)	159.40
Peptide **2**			
N1–H1···O1^{iii}	2.03	2.908(6)	173.71
N2–H2···O13^{iv}	1.98	2.854(5)	175.02
O2–H2···O4^{iii}	1.83	2.620(5)	155.73
N5–H5···O6^{v}	2.03	2.898(6)	168.24
N6–H6···O3^{vi}	1.98	2.854(5)	169.60
O11–H11···O9^{vii}	1.83	2.626(5)	157.50
N3–H3···O12^{viii}	2.13	2.941(5)	152.60
N4–H4···O8^{ix}	2.00	2.874(5)	172.50
O7–H7···O14^{viii}	1.81	2.609(5)	159.30
Peptide **4**			
N2–H2···O3^{i}	2.11	2.964(2)	162.30
N3–H3···O4^{i}	2.11	2.956(2)	160.40

Symmetry codes: (i) $x-1, y, z$; (ii) $1-x, y-1/2, 1/2-z$; (iii) $2-x, -y, 2-z$; (iv) $1+x, y, z$; (v) $x-1, 1+y, z$; (vi) $x-1, y, z$; (vii) $x-1, y+1, z$; (viii) $1+x, y-1, z$; (ix) $2-x, 1-y, 1-z$.

ABA units of two neighboring molecules could recognize each other through intermolecular H-bonds (*Fig. 7* and *Table 3*). The arrangement was further stabilized by two additional intermolecular H-bonds between the carboxylic OH and the Boc C=O groups, to create a molecular duplex. These duplexes were further inter-linked

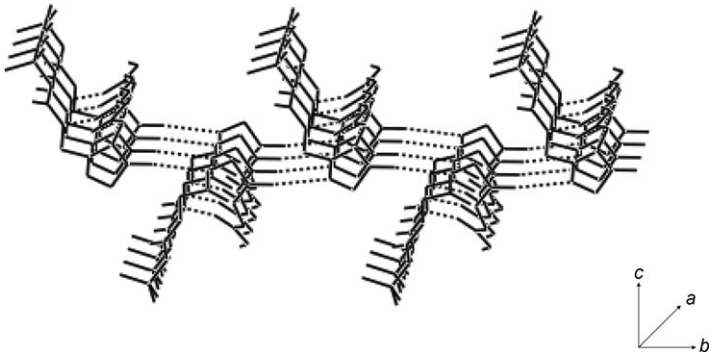

Fig. 5. *Packing diagram of peptide* **1** *showing the formation of corrugated* β*-sheets parallel to the crystallographic* b*-axis.* Side chains of amino acids are omitted for clarity. The dotted lines indicate H-bonding.

through two intermolecular H-bonds between the β-Ala C=O and the β-Ala NH groups to create a layer of β-sheets (*Fig. 7*). Several such parallel layers were stacked one on top of the other and linked through *Van der Waals* interactions (*Fig. 8*). We were unable to grow single crystals of Boc-γ-Abu-*m*-ABA (**3**). However, since both **2** and **3** are structurally similar, the latter is expected to produce a β-sheet-like structure as observed in the solid state structure of **2**. This hypothesis is supported by the FT-IR data (*Table 1* and *Fig. 2*).

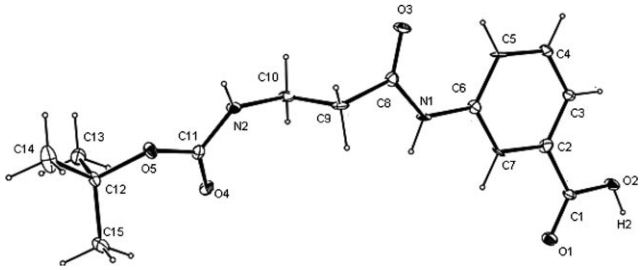

Fig. 6. *ORTEP Diagram of peptide* **2** *with atom-numbering scheme.* Thermal ellipsoids are drawn at the 25% probability level.

The colorless, monoclinic crystals of peptide **4** were obtained from a MeOH/H_2O mixture by slow evaporation. The space group was $P2_1$ with one molecule in the asymmetric unit. The crystal structure of **4** (*Fig. 9*), where the *m*-ABA of **2** has been replaced by *m*-NA, showed an infinite ribbon-like β-sheet structure through intermolecular H-bonding (*Fig. 10*). The backbone torsion angles, which characterize the extended conformation, were ϕ_1, −136.4(2)°; θ_1, 173.4(2)°; and ψ_1, 140.1(2)° at β-Ala (*Table 2*). The incorporation of β-Ala helped to attain a fully extended conformation, which was necessary for β-sheet formation. There were two intermolecular H-bonds between N2 and O3 ($x-1, y, z$) and between N3 and O4 ($x-1, y, z$) with donor–accepter distances of 2.964 and 2.956 Å, respectively (*Table 3*). These H-bonds resulted in the formation of a 14-membered ring that connects neighboring

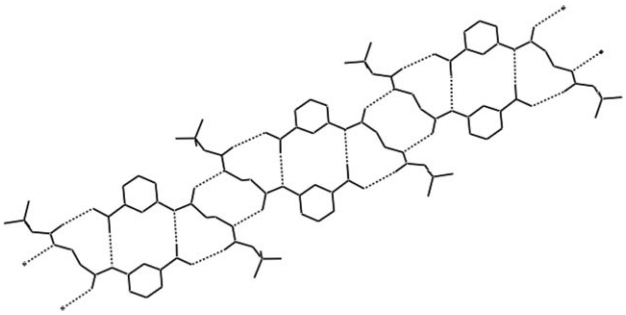

Fig. 7. *Packing diagram of peptide* **2** *showing the formation of a β-sheet layer through the antiparallel self-assembly of peptides.* The dotted lines indicate H-bonding.

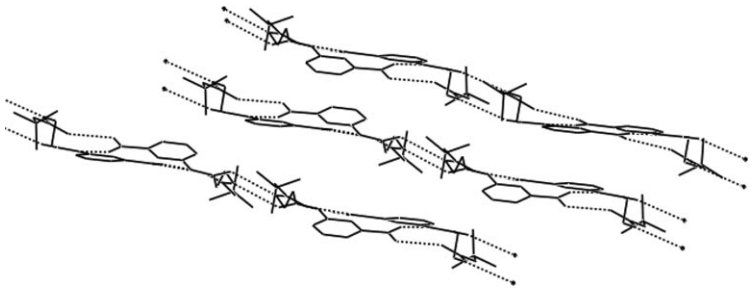

Fig. 8. *Packing diagram of peptide* **2** *showing the stacking of parallel layers of β-sheets through* Van der Waals *interactions*

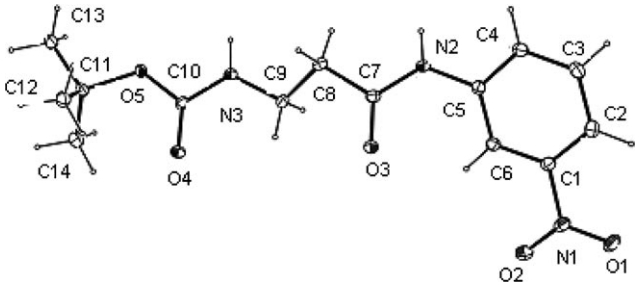

Fig. 9. *ORTEP Diagram of peptide* **4** *with atom-numbering scheme.* Thermal ellipsoids are drawn at the 25% probability level.

molecules. A parallel β-pleated sheet parallel to the crystallographic *a*-axis was thus formed with the strands running in the same direction (*Fig. 10*). It is interesting that the space group was $P2_1$ with just one molecule in the unit cell, which facilitated this packing formation. The molecular arrangement was further stabilized by $\pi-\pi$ interactions between the phenyl rings. It is a well-documented fact that $\pi-\pi$ interactions have a significant role to play in amyloid aggregation [37]. The peptide **5**, Boc-γ-Abu-*m*-NA, where the β-Ala of **4** was replaced by γ-Abu, was expected to

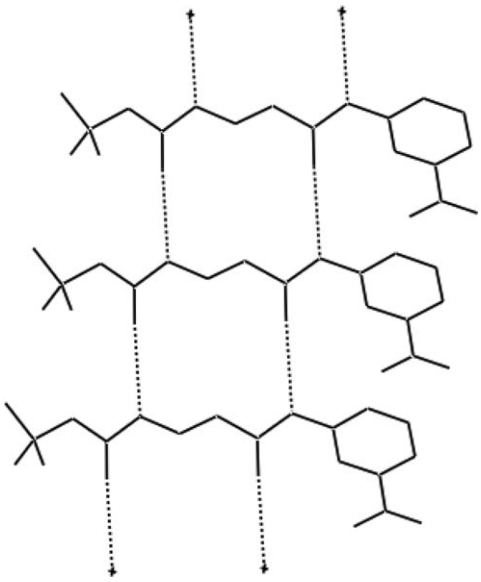

Fig. 10. *Packing diagram of peptide* **4** *showing the formation of a ribbon-like* β*-sheet through H-bonding and* $\pi-\pi$ *interactions*

adopt a similar ribbon-like β-sheet structure in the solid state like that of **4**. Although it was not possible to grow single crystals of **5**, the FT-IR data indicated a β-sheet-like structure in the solid state (*Table 1*). These studies clearly demonstrate that, although the self-assembling patterns for peptides **1**, **2**, and **4** in the solid state are significantly different, all of them form layers of β-sheets through different kinds of two-dimensional H-bonding networks.

Scanning Electron-Microscopic Study. Field-emission scanning electron-microscopic (FE-SEM) images of the dried fibrous materials of peptides **1**–**5**, grown slowly from acetone, clearly demonstrated that the aggregates in the solid state were bunches of fibrillar structures (*Fig. 11*). Peptides **2** and **3**, with free COOH groups, showed excellent fibril-forming properties. Peptides **4** and **5**, having NO_2 in place of COOH groups, could also produce fibrillar structures. Interestingly, the peptide fibrils generated from **2** and **3** exhibited an amyloid-like behavior, as they bind to the physiological dye Congo red (*Fig. 12*). These results demonstrate that supramolecular β-sheet forming small peptides with diverse functionalities could promote fibrillar structures in the solid state.

Conclusions. – Solid-state FT-IR data for all peptides revealed that they self-assemble to form intermolecular H-bonded supramolecular β-sheet structures. Single crystal X-ray diffraction studies showed that although peptides **1**, **2**, and **4** are structurally different, all of them formed β-sheet-like structures through molecular self-assembly. While the bent structure of **1** self-assembled into a β-sheet-like structure, the extended structure of **2** formed a β-sheet layer through the self-association of molecular duplexes. The preferred structure of **4** was an infinite ribbon-like β-sheet

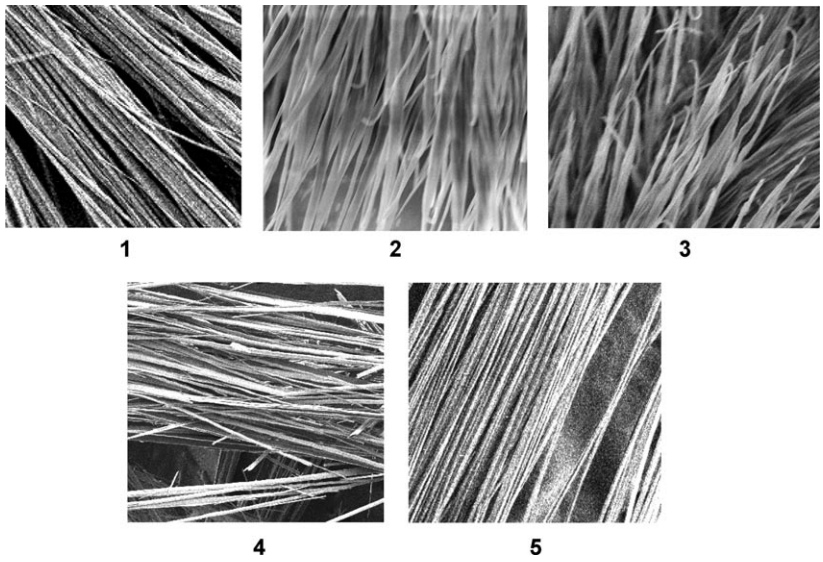

Fig. 11. *FE-SEM Images of the fibrous materials of peptides* **1**–**5** *showing the formation of the fibrillar structures*

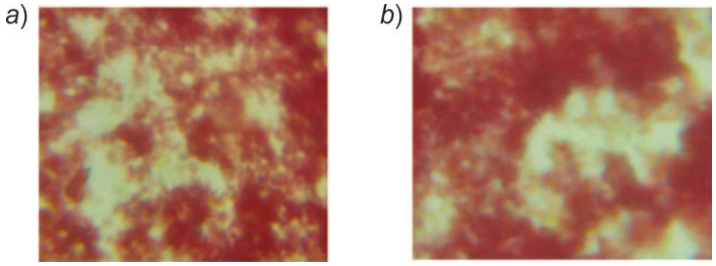

Fig. 12. *Light microscope images* (× 1000 magnification) *of Congo red stained fibrils of* a) *peptide* **2** *and* b) *peptide* **3**, *a characteristic feature of amyloid fibrils*

structure through molecular self-assembly. SEM studies revealed that the peptides **1**–**5** could form fibrillar structures in the solid state. The fibrils grown from **2** and **3** were found to bind with the physiological dye Congo red, a characteristic feature of amyloid fibrils. The insertion of ω-amino acids, such as β-Ala and γ-Abu, into the peptide backbone not only helped to form H-bonded supramolecular β-sheet structures, but also provided proteolytic resistance by replacing regular peptide bonds with C–C bonds. The investigation of the pathway(s) of amyloid-fibril formation has a major role in therapeutics of the amyloid diseases. In this context, developing easily modifiable molecular systems that will self-assemble to amyloid-like fibrils is very important. The amyloid-like fibrils generated from the small peptides **1**–**5** may serve as screening tools in the search for anti-neurodegenerative drugs acting as inhibitors of misfolded protein aggregation.

The financial assistance of the *UGC*, New Delhi is acknowledged (Major Research Project, No. 32-190/2006 (SR)). *A. D.* thanks the *UGC*, New Delhi, India, for providing her a senior research fellowship, and *E. C. S.* thanks the *EPSRC* for funding.

Experimental Part

General. Column chromatography (CC): silica gel (SiO_2; 100–200 mesh; *Spectrochem*, India). IR Spectra: *Perkin Elmer 782* FT-IR spectrometer; $\tilde{\nu}$ in cm^{-1}. ^{1}H- and ^{13}C-NMR Spectra: *Bruker Avance 300* NMR spectrometer, at 300 and 75 MHz, resp.; δ in ppm, J in Hz; peptide concentrations 1–10 and 30–40 mM for ^{1}H- and ^{13}C-NMR, resp.

Peptide Synthesis. Peptides **1**–**5** were synthesized by conventional soln.-phase procedures [38]. Boc and Me ester groups were used to protect the NH_2 and COOH groups, resp., and dicyclohexylcarbodiimide (DCC) and 1-hydroxybenzotriazole (HOBT) were employed as coupling agents. Methyl ester hydrochlorides of Aib, Ile, and *m*-ABA were prepared by the $SOCl_2$-MeOH procedure. The purities of all intermediates obtained were checked by TLC on silica gel (SiO_2) and used without further purification. The final peptide products were purified by CC (SiO_2; AcOEt/petroleum ether (PE)). Peptides **1**–**5** were fully characterized by IR, ^{1}H- and ^{13}C-NMR. Moreover, the structures of peptides **1**, **2**, and **4** were confirmed by X-ray diffraction analysis.

Boc-Ile-Aib-Ile-OMe (**1**). Boc-Ile-Aib-OH [6] (1.0 g, 3.16 mmol) was dissolved in DMF (3 ml). Ile-OMe (0.46 g, 3.16 mmol), obtained from the corresponding HCl salt, was added, followed by the addition of DCC (0.65 g, 3.16 mmol). The mixture was stirred at r.t. for 5 d. The precipitated dicyclohexylurea (DCU) was filtered and diluted with AcOEt. The org. layer was washed with an excess of H_2O, 1M HCl (3×30 ml), 1 M Na_2CO_3 soln. (3×30 ml), and then again with H_2O. The filtrate was then dried (Na_2SO_4) and evaporated *in vacuo* to give a light yellow solid. Purification was performed by CC (SiO; AcOEt/PE). Single crystals of **1** were grown from acetone/H_2O 9:1 by slow evaporation and were stable at r.t. (1.29 g, 92%). M.p. 77–78°. IR (KBr): 1523, 1667, 1712, 3320, 3387. ^{1}H-NMR ($CDCl_3$): 0.90–0.97 (*m*, 12 H, Me(γ), Me(δ) of Ile); 1.14–1.22 (*m*, 4 H, $CH_2(\gamma)$ of Ile); 1.46 (*s*, 3 Me of Boc); 1.59 (*s*, 2 Me(β) of Aib); 1.86–1.92 (*m*, 2 H, H–C(β) of Ile); 3.75 (*s*, MeO); 3.87–3.90 (*m*, H–C(α) of Ile(1)); 4.53–4.62 (*m*, H–C(α) of Ile(3)); 5.02 (*d*, J = 6.9, NH of Ile(1)); 6.55 (*s*, NH of Aib); 7.10 (*d*, J = 8.4, NH of Ile(3)). ^{13}C-NMR ($CDCl_3$): 11.3; 11.5; 15.4; 15.5; 24.7; 24.8; 25.1; 25.5; 28.2; 36.9; 37.7; 51.9; 56.7; 57.5; 59.8; 80.2; 155.8; 171.5; 172.2; 173.8. Anal. calc. for $C_{22}H_{41}N_3O_6$ (443.57): C 59.57, H 9.32, N 9.48; found: C 59.52, H 9.28, N 9.52.

Boc-β-Ala-m-*ABA* (**2**). Boc-β-Ala-*m*-ABA-OMe [4] (1.0 g, 3.10 mmol) was dissolved in MeOH (15 ml), and 2M NaOH (10 ml) was then added. The mixture was stirred at r.t. for 2 d. The progress of the reaction was monitored by TLC. After completion of the reaction, MeOH was evaporated. The residue obtained was diluted with H_2O and washed with Et_2O. The aq. layer was neutralized with 2M HCl and then extracted with AcOEt. The solvent was evaporated *in vacuo* to give a light yellow solid. Purification was performed by CC (SiO; AcOEt/PE). Single crystals of **2** were grown by slow evaporation from acetone/toluene and were stable at r.t. (0.76 g, 80%). M.p. 182–184°. IR (KBr): 1535, 1689, 3200, 3343. ^{1}H-NMR ((D$_6$)DMSO): 1.33 (*s*, 3 Me of Boc); 2.44 (*t*, J = 6.9, $CH_2(\beta)$ of β-Ala); 3.19 (*q*, J = 6.6, $CH_2(\alpha)$ of β-Ala); 6.84–6.91 (*m*, NH of β-Ala); 7.37 (*t*, J = 7.8, H–C(5) of *m*-ABA); 7.57 (*d*, J = 7.5, H–C(4) of *m*-ABA); 7.76 (*d*, J = 7.8, H–C(6) of *m*-ABA); 8.20 (*s*, H–C(2) of *m*-ABA); 10.01 (*s*, NH of *m*-ABA). ^{13}C-NMR ((D$_6$)DMSO): 28.7; 36.9; 37.3; 78.1; 123.7; 124.4; 129.3; 131.7; 139.8; 156.0; 167.7; 170.1. Anal. calc. for $C_{15}H_{20}N_2O_5$ (308.32): C 58.42, H 6.53, N 9.08; found: C 58.30, H 6.39, N 8.88.

Boc-γ-Abu-m-*ABA* (**3**). From Boc-γ-Abu-*m*-ABA-OMe, **3** was synthesized following a similar procedure to that of **2**. Yield: 0.94 g (82%). M.p. 172–174°. ^{1}H-NMR ((D$_6$)DMSO): 1.23 (*s*, 3 Me of Boc); 1.51–1.60 (*m*, $CH_2(\beta)$ of γ-Abu); 2.17 (*t*, J = 7.2, $CH_2(\alpha)$ of γ-Abu); 2.82 (*q*, J = 6.6, $CH_2(\gamma)$ of γ-Abu); 6.70–6.80 (*m*, NH of γ-Abu); 7.27 (*t*, J = 7.8, H–C(5) of *m*-ABA); 7.47 (*d*, J = 7.5, H–C(4) of *m*-ABA); 7.67 (*d*, J = 7.7, H–C(6) of *m*-ABA); 8.09 (*s*, H–C(2) of *m*-ABA); 9.95 (*s*, NH of *m*-ABA). ^{13}C-NMR ((D$_6$)DMSO): 25.9; 28.7; 34.3; 39.9; 77.9; 120.3; 123.6; 124.3; 129.4; 131.7; 139.9; 156.1; 167.7; 171.7. Anal. calc. for $C_{16}H_{22}N_2O_5$ (322.35): C 59.61, H 6.87, N 8.69; found: C 59.75, H 6.99, N 8.85.

Boc-β-Ala-m-*NA* (**4**). Boc-β-Ala-OH (0.95 g, 5 mmol) was dissolved in DMF (3 ml), and *m*-nitroaniline (*m*-NA; 0.68 g, 5 mmol) was added, followed by DCC (1.0 g, 5 mmol). The mixture was stirred at r.t. for 3 d. The precipitated DCU was filtered and diluted with AcOEt (40 ml). The org. layer was washed with an excess of H_2O, 1M HCl (3 × 30 ml), 1M Na_2CO_3 soln. (3 × 30 ml), and then again with H_2O. The solvent was then dried (anh. Na_2SO_4) and evaporated *in vacuo*, giving **4** as a brown solid (1.32 g, 85%). Single crystals were grown by slow evaporation from MeOH/H_2O and were stable at r.t. M.p. 155–156°. IR (KBr): 1546, 1696, 3326. ^{1}H-NMR ($CDCl_3$): 1.44 (*s*, 3 Me of Boc); 2.69–2.75 (*m*, $CH_2(\beta)$ of β-Ala); 3.54–3.60 (*m*, $CH_2(\alpha)$ of β-Ala); 5.37 (br. *s*, NH of β-Ala); 7.47 (*t*, *J* = 8.1, H–C(5) of *m*-NA); 7.91–7.97 (*m*, H–C(4), H–C(6) of *m*-NA); 8.51 (*s*, H–C(2) of *m*-NA); 9.12 (br. *s*, NH of *m*-NA); ^{13}C-NMR ($CDCl_3$): 28.3; 36.4; 37.8; 80.1; 114.5; 118.6; 125.4; 129.7; 139.3; 148.4; 156.7; 170.3. Anal. calc. for $C_{14}H_{19}N_3O_5$ (309.32): C 54.36, H 6.19, N 13.58; found: C 54.18, H 6.04, N 13.43.

Boc-γ-Abu-m-*NA* (**5**). Peptide **5** was synthesized following a similar procedure to that of peptide **4**. Yield: 1.41 g (87%). IR (KBr): 1532, 1680, 3303, 3357. ^{1}H-NMR ($CDCl_3$): 1.47 (*s*, 3 Me of Boc); 2.03–2.09 (*m*, $CH_2(\beta)$ of γ-Abu); 2.43–2.55 (*m*, $CH_2(\alpha)$ of γ-Abu); 3.26–3.35 (*m*, $CH_2(\gamma)$ of γ-Abu); 4.91–5.50 (*m*, NH of γ-Abu); 7.45 (*t*, *J* = 7.5, H–C(5) of *m*-NA); 7.91 (*d*, *J* = 7.2, H–C(4) of *m*-NA); 8.01 (*d*, *J* = 6.9, H–C(6) of *m*-NA); 8.55 (*s*, H–C(2) of *m*-NA); 9.77 (br. *s*, NH of *m*-NA). ^{13}C-NMR ($CDCl_3$): 27.6; 28.4; 34.6; 39.1; 80.3; 114.5; 118.3; 125.4; 129.6; 139.8; 148.6; 157.8; 171.8. Anal. calc. for $C_{15}H_{21}N_3O_5$ (323.34): C 55.71, H 6.54, N 12.99; found: C 55.56, H 6.38, N 12.87.

Field-Emission Scanning-Electron Microscopy. The morphologies of the peptides **1**–**5** were investigated using field-emission scanning electron microscopy. For the study, fibrous materials were dried and gold coated. The micrographs were taken with a *JEOL JSM 6700F* apparatus.

Congo Red-Binding Study. The fibrils generated from peptides **2** and **3** were stained with alkaline Congo red soln. (MeOH/glass dist. H_2O 8:2, containing 10 µl of 1% NaOH) for 2 min and then the excess stain was removed by rinsing the stained fibrils with MeOH/glass dist. H_2O 8:2 several times. The stained fibrils were dried *in vacuo* at r.t. for 24 h and then visualized under a light microscope at × 1000 magnification [39–42].

Single-Crystal X-Ray Diffraction Study. Single crystals of **1**, **2**, and **4** were obtained by slow evaporation from acetone/H_2O 9:1, acetone/toluene 9:1, and MeOH/H_2O 9:1, resp. Data for **1**, **2**, and **4**

Table 4. *Crystallographic Refinement Details for Peptides* **1**, **2**, *and* **4**

	1	**2**	**4**
Formula	$C_{22}H_{41}N_3O_6$	$C_{15}H_{20}N_2O_5$	$C_{14}H_{19}N_3O_5$
Formula weight [g mol^{-1}]	443.58	308.33	309.32
Crystal System	Orthorhombic	Triclinic	Monoclinic
Space group	$P2_12_12_1$	$P\bar{1}$	$P2_1$
Z	4	6	2
a [Å]	9.2700(2)	10.798(2)	5.0378(3)
b [Å]	12.0462(3)	13.490(2)	26.274(1)
c [Å]	23.2439(5)	17.694(3)	5.5682(3)
α [°]	90	82.535(3)	90
β [°]	90	82.003(3)	96.056(2)
γ [°]	90	75.588(3)	90
V [Å^3]	2595.6(1)	2460.0(7)	732.92(7)
μ (MoK_α) [mm^{-1}]	0.082	0.094	0.108
Collected reflections	18634	17410	4692
Unique reflections	5666	7719	2845
No. Parameters	290	604	202
R_{int}	0.0343	0.0809	0.0231
GoF	1.052	1.077	1.060
R_1 [$I > 2\sigma(I)$]	0.0531	0.0908	0.0363
ωR_2 [$I > 2\sigma(I)$]	0.1336	0.1509	0.0946

were collected at 120(2) K with graphite monochromated X-radiation on *Bruker SMART* diffractometers (*SMART 6K* for **1** and **4**, and *SMART 1K* for **2**). Data processing was performed with standard *Bruker* software [43]. Structure solution was by direct methods and refinement was on F^2 using full-matrix least-squares techniques. All H-atoms were placed at calculated positions and had been refined with a riding model. All non-H-atoms were refined anisotropically (see *Table 4* for further crystallographic details). The crystallographic data of **1**, **2**, and **4** have been deposited with the *Cambridge Crystallographic Data Centre* as supplementary publication numbers CCDC-673918–CCDC-673920 and can be obtained free of charge *via* http://www.ccdc.cam.ac.uk/data_request/cif.

REFERENCES

[1] A. Dutt, M. G. B. Drew, A. Pramanik, *Tetrahedron* **2008**, *64*, 549.
[2] D. Haldar, M. G. B. Drew, A. Banerjee, *Tetrahedron* **2006**, *62*, 6370.
[3] A. K. Das, A. Banerjee, M. G. B. Drew, S. Ray, D. Haldar, A. Banerjee, *Tetrahedron* **2005**, *61*, 5027.
[4] A. Dutt, M. G. B. Drew, A. Pramanik, *Org. Biomol. Chem*. **2005**, *3*, 2250.
[5] S. K. Kundu, P. A. Mazumdar, A. K. Das, V. Bertolasi, A. Pramanik, *J. Chem. Soc., Perkin Trans. 2* **2002**, 1602.
[6] A. Dutt, A. Dutta, R. Mondal, E. C. Spencer, J. A. K. Howard, A. Pramanik, *Tetrahedron* **2007**, *63*, 10282.
[7] A. Banerjee, A. K. Das, M. G. B. Drew, A. Banerjee, *Tetrahedron* **2005**, *61*, 5906.
[8] A. Banerjee, S. K. Maji, M. G. B. Drew, D. Haldar, A. K. Das, A. Banerjee, *Tetrahedron* **2004**, *60*, 5935.
[9] S. K. Maji, A. Banerjee, M. G. B. Drew, *Chem. Commun*. **2001**, 1946.
[10] S. Ray, A. K. Das, M. G. B. Drew, A. Banerjee, *Chem Commun*. **2006**, 4230.
[11] O. Rathore, D. Y. Sogah, *J. Am. Chem. Soc.* **2001**, *123*, 5231.
[12] S. Vauthey, S. Santoso, H. Gong, N. Watson, S. Zhang, *Proc. Natl. Acad. Sci. U.S.A.* **2002**, *99*, 5355.
[13] O. N. Antzutkin, J. J. Balbach, R. D. Leapman, N. W. Rizzo, J. Reed, R. Tycko, *Proc. Natl. Acad. Sci. U.S.A.* **2000**, *97*, 13045.
[14] W. Wang, M. H. Hecht, *Proc. Natl. Acad. Sci. U.S.A.* **2002**, *99*, 2760.
[15] D. J. Pochan, J. P. Schneider, J. Kretsinger, B. Ozbas, K. Rajagopal, L. Haines, *J. Am. Chem. Soc.* **2003**, *125*, 11802.
[16] M. S. Lamm, K. Rajagopal, J. P. Schneider, D. J. Pochan, *J. Am. Chem. Soc.* **2005**, *127*, 16692.
[17] H. Yokoi, T. Kinoshita, S. Zhang, *Proc. Natl. Acad. Sci. U.S.A.* **2005**, *102*, 8414.
[18] H. A. Lashuel, S. R. LaBrenz , L. Woo, L. C. Serpell, J. W. Kelly, *J. Am. Chem. Soc.* **2000**, *122*, 5262.
[19] S. Deechongkit, E. T. Powers, S. L. You, J. W. Kelly, *J. Am. Chem. Soc.* **2005**, *127*, 8562.
[20] M. G. Ryadnov, D. N. Woolfson, *J. Am. Chem. Soc.* **2005**, *127*, 12407.
[21] E. D. Sone, S. I. Stupp, *J. Am. Chem. Soc.* **2004**, *126*, 12756.
[22] A. Aggeli, M. Bell, N. Boden, J. N. Keen, P. F. Knowles, T. C. B. Mcleish, M. Pitkeathly, S. E. Radford, *Nature* **1997**, *386*, 259.
[23] T. C. Holmes, S. de Lacalle, X. Su, G. Liu, A. Rich, S. Zhang, *Proc. Natl. Sci. U.S.A.* **2000**, *97*, 6728.
[24] J. Kisiday, M. Jin, B. Kurz, H. Huang, C. Semino, S. Zhang, A. J. Grodzinsky, *Proc. Natl. Acad. Sci. U.S.A.* **2002**, *99*, 9996.
[25] G. Taubes, *Science* **1996**, *271*, 1493.
[26] P. T. Lansbury, *Acc. Chem. Res.* **1996**, *29*, 317.
[27] J.-C. Rochet, P. T. Lansbury, *Curr. Opin. Struct. Biol*. **2000**, *10*, 60.
[28] D. M. Walsh, A. Lomakin, G. B. Benedek, M. M. Condron, D. B. Teplow, *J. Biol. Chem*. **1997**, *272*, 22364.
[29] M. Baba, S. Nakajo, P. H. Tu, T. Tomita, K. Nakaya, V. M. Y. Lee, J. Q. Trojanowski, T. Iwatsubo, *Am. J. Pathol*. **1998**, *152*, 879.
[30] M. G. Spillantini, R. A. Crowther, R. Jakes, M. Hasegawa, M. Goedert, *Proc. Natl. Acad. Sci. U.S.A.* **1998**, *95*, 6469.
[31] K. M. Pan, M. Baldwin, J. Nguyen, M. Gasset, A. Serban, D. Groth, I. Mehlhorn, Z. Huang, R. J. Fletterick, F. E. Cohen, *Proc. Natl. Acad. Sci. U.S.A.* **1993**, *90*, 10962.

[32] S. B. Prusiner, *Proc. Natl. Acad. Sci. U.S.A.* **1998**, *95*, 13363.
[33] A. Banerjee, P. Balaram, *Curr. Sci.* **1997**, *73*, 1067.
[34] C. Toniolo, M. Palumbo, *Biopolymers* **1977**, *16*, 219.
[35] M. Mutter, F. Maser, K.-H. Altman, C. Toniolo, G. M. Bonora, *Biopolymers* **1985**, *24*, 1057.
[36] V. Moretto, M. Crisma, G. M. Bonora, C. Toniolo, H. Balaram, P. Balaram, *Macromolecules* **1989**, *22*, 2939.
[37] E. Gazit, *FASEB J.* **2002**, *16*, 77.
[38] M. Bodanszky, A. Bodanszky, 'The Practice of Peptide Synthesis', Springer-Verlag, New York, 1984.
[39] Y.-S. Kim, T. W. Randolph, M. C. Manning, F. J. Stevens, J. F. Carpenter, *J. Biol. Chem.* **2003**, *278*, 10842.
[40] A. Lim, A. M. Makhov, J. Bond, H. Inouye, L. H. Connors, J. D. Griffith, B. W. Erickson, D. A. Kirschner, C. E. Costello, *J. Struct. Biol.* **2000**, *130*, 363.
[41] R. Azriel, E. Gazit, *J. Biol. Chem.* **2001**, *276*, 34156.
[42] E. W. Klunk, J. W. Pettegrew, D. J. Abraham, *J. Histochem. Cytochem.* **1989**, *37*, 1293.
[43] Bruker SMART-NT version 5.0 (data collection), SAINT version 6.04 (data processing), and SHELXTL version 6.1 (structure solution, refinement), Bruker AXS Inc., Madison, Wisconsin, USA, 1998.

Received March 2, 2009